The Journal of Neuroscience, August 1995, 15(8): 5560–5573

Repeated Confocal Imaging of Individual Dendritic Spines in the Living Hippocampal Slice: Evidence for Changes in Length and Orientation Associated with Chemically Induced LTP

Toshiyuki Hosokawa,[1] Dmitri A. Rusakov,[2,3] T. V. P. Bliss,[4] and Alan Fine[1]

[1]Department of Physiology and Biophysics and Institute for Neuroscience, Dalhousie University Faculty of Medicine, Halifax, Nova Scotia B3H 4H7, Canada, [2]Biology Department, The Open University, Milton Keynes MK7 6AA, United Kingdom, [3]Bogomoletz Institute of Physiology, Kiev 252601, Ukraine, and [4]Division of Neurophysiology and Neuropharmacology, National Institute for Medical Research, London NW7 1AA, United Kingdom

Using confocal microscopy in conjunction with microdrop application of DiI, we have imaged and measured individual dendritic spines of living hippocampal CA1 pyramidal neurons in acute brain slices, before and approximately 3 hr after induction of long-term potentiation by chemical means. Statistical analysis of changes in the length of individual spines, and comparison with results of Monte Carlo simulations, suggests that two forms of structural change occur in chemically induced long-term potentiation: growth of a subpopulation of small spines, and angular displacement of spines. These changes could provide a structural basis for the expression of long-term potentiation.

[Key words: long-term potentiation, synaptic plasticity, learning and memory, DiI, fluorescence, Monte Carlo simulation]

Dendritic spines receive the majority of excitatory synaptic connections in the mammalian CNS (Colonier, 1968). Since Ramon y Cajal's first description of dendritic spines more than a century ago (1891), evidence has accumulated that the shape or density of spines may be altered by a range of developmental, pathological and experimental influences. Thus, for example, dendritic spines are known to regress and regrow in response to deafferentation and reinnervation (Kemp and Powell, 1971; Parnavelas et al., 1974; Matthews et al., 1976; Caceres and Steward, 1983; Ingham et al., 1989) or to the onset and cessation of epileptic seizures (Scheibel et al., 1974; Isokawa and Levesque, 1991; Müller et al., 1993). Modulation of dendritic spine number and morphology has also been observed in response to exogenous gonadal steroids (Gould et al., 1990) and throughout the normal estrous cycle (Wooley et al., 1990).

Ramon y Cajal (1911), Hebb (1949), Eccles (1965), and others since have suggested that alterations in spine number or shape could provide a mechanism for the storage of memories, by strengthening or weakening particular synaptic connections in response to experience. Evidence of such alterations has been found in fixed CNS tissue from animals of several species reared in complex versus simple environments, or exposed to various training or stimulation regimens (reviewed by Globus, 1975; Greenough and Bailey, 1988; Bailey and Kandel, 1993; Horner, 1993; Harris and Kater, 1994). Changes in dendritic spines after induction of long-term potentiation (LTP), a widely studied experimental model of learning (Bliss and Lømo, 1973; Bliss and Collingridge, 1993), have been reported by a number of investigators (e.g., Van Harreveld and Fifkova, 1975; Fifkova and Van Harreveld, 1977; Lee et al., 1979, 1980; Desmond and Levy, 1983, 1986a,b; Chang and Greenough, 1984; Petukhov and Popov, 1986; Schuster et al., 1990; Geinisman et al., 1991, 1992b; Wallace et al., 1991). Indeed, the long duration of LTP (Bliss and Gardner-Medwin, 1973; Racine et al., 1983) suggests a structural basis for its maintained expression.

Until now, it has not been possible to visualize individual CNS synapses throughout the course of learning or potentiation: all previous studies of changes in synaptic morphology have been correlational, comparing average numbers and dimensions of spines in potentiated and unpotentiated brain tissue after fixation. Interpretation of such studies has been complicated by the great variability of synaptic morphologies, with attendant problems of sampling, as well as by potential artifacts stemming from fixation and sectioning; as remarked by Lisman and Harris (1993), "it would clearly be of great interest to visualize individual synapses as they undergo LTP and ask directly whether both pre- and postsynaptic growth occurs."

With this objective in mind, we developed methods for the repeated imaging of dendritic spines in living, electrically monitored brain slices. Small groups of neurons can be stained by brief application of lipophilic fluorescent dyes in oil-microdrops, rapidly yielding Golgi-like staining of dendritic spines and presynaptic terminals. With the use of confocal microscopy (Minsky, 1957; Fine et al. 1988), these labeled synaptic structures can be clearly and unambiguously visualized even tens of micrometers within the living slice, during concurrent electrophysiological recording. By successively imaging the same living cells, we previously demonstrated the persistence of individual spines of hippocampal neurons over periods of 5 hr or longer (Hosokawa et al., 1992). We have now used these optical methods to determine whether the dimensions of individual spines change over time; here, we report increases in spine reorientation

Received Sept. 29, 1994; revised Mar. 6, 1995; accepted Mar. 14, 1995.

We thank Ms. Cindee Leopold for technical assistance, and Dr. R. M. Douglas for providing A/DVANCE data acquisition and analysis software. This work was supported by grants from the Human Frontier Science Program, NATO, the Whitaker Foundation, the BBSRC and the Medical Research Council (UK). T.H. was a postdoctoral fellow of the Human Frontier Science Program.

Correspondence should be addressed to Alan Fine at the above address.

Copyright © 1995 Society for Neuroscience 0270-6474/95/155560-14$05.00/0

and in the length of a specific population of spines following chemically induced LTP.

Preliminary aspects of this research have been presented in abstract form (Fine et al., 1991).

Materials and Methods

Tissue preparation. Hippocampal slices were prepared from male Sprague–Dawley rats between 3 and 4 weeks of age. Rats were anesthetized with ketamine and then decapitated. Brains were removed rapidly and submerged briefly in ice-cold oxygenated calcium-free artificial cerebrospinal fluid (0Ca-ACSF) containing 120 mM NaCl, 3 mM KCl, 1.2 mM NaH_2PO_4, 23 mM $NaHCO_3$, 2.4 mM $MgCl_2$, and 11 mM D-glucose, pH 7.3. The brain was then quickly blocked, glued to the stage of a vibrating microtome (Campden Instruments) and again covered with ice-cold 0Ca-ACSF. Transverse hippocampal slices, 400 μm thick, were cut and transferred to a glass-bottomed controlled-temperature recording chamber on the mechanical stage of an upright compound microscope (Leitz Ortholux) mounted beneath a confocal laser scanning and imaging head (Bio-Rad MRC-500 modified with high-reflectivity mirrors). Within the chamber, the slices were continuously superfused at 35°C with standard ACSF (120 mM NaCl, 3 mM KCl, 1.2 mM NaH_2PO_4, 23 mM $NaHCO_3$, 1.2 mM $MgCl_2$, 2.4 mM $CaCl_2$, and 11 mM D-glucose, pH 7.3) or potentiation medium (see below) saturated with 95% O_2, % CO_2. Unless otherwise indicated, all chemicals were supplied by Sigma, Canada.

Labeling of dendritic spines. Mono-unsaturated DiI (1,1′-dioleyl-3,3,3′,3′-tetramethylindocarbocyanine methanesulfonate) (Honig and Hume, 1986; Thanos and Bonhoeffer, 1987; O'Rourke and Fraser, 1990) was applied to the surface of the hippocampal slice via oil microdrops (Hosokawa et al., 1992). DiI (Molecular Probes, Oregon) was dissolved in fresh cod liver oil (Westcan, Canada) to a final concentration of 10 μg/μl by heating in a boiling water bath with agitation. The tip of a blunt (5–10 μm tip diameter) micropipette was back-filled with this solution, after which the micropipette was connected to a 10 ml syringe via polyethylene tubing and a three-way stopcock, and mounted in a micromanipulator fixed to the confocal microscope stage. Using a 2.5× objective with transmitted light, the pipette tip was positioned over the stratum pyramidale of area CA1, and a droplet of dye, 50–100 μm diameter, was expressed under pressure. The pipette was advanced until the droplet contacted the tissue surface; the pipette was then withdrawn, leaving the adherent droplet in place. This procedure was repeated at several sites approximately 200 μm apart along the CA1 stratum pyramidale (Fig. 1*A*). After approximately 20 min, excess dye was removed by suction with a larger micropipette (30–50 μm tip diameter), or was dispersed by momentarily lowering the fluid level in the chamber (Fig. 1*B*).

Electrical recording. Evoked field responses in area CA1 were recorded prior to DiI application; slices displaying abnormal responses (e.g., continued afterdischarges, compound spikes) at any time during the experiment were discarded. Brief biphasic constant-current stimuli (50 μsec duration) were applied via an insulated, sharpened tungsten electrode (A-M Systems, Everett, WA) in stratum radiatum; responses were recorded via an ACSF-filled extracellular micropipette also positioned within the stratum radiatum of CA1. Both electrodes were mounted on hydraulic micromanipulators attached to the microscope mechanical stage. Electrodes were removed during DiI application and while searching for suitably labeled cells (see below), and then replaced close to the area selected for imaging. Stimulus strength was adjusted to yield half-maximal response amplitudes, and stimuli were delivered once each 30 sec. Slope and amplitude of the field excitatory postsynaptic potential (fEPSP) were calculated and displayed on line using A/DVANCE software (FST, Vancouver); slices with unstable fEPSPs were rejected.

Confocal microscopy of fluorescent cells. Labeled cells and processes within 75 μm of the upper surface of the slice were imaged by laser-scanning confocal microscopy as previously described (Hosokawa et al., 1994), using a 40× water-immersion objective (Zeiss, n.a. 0.75). To identify non-viable cells, ethidium bromide (2 μg/ml) was present in the ACSF at all times; this fluorescent nuclear marker is excluded from healthy cells (Fig. 1*C*). Dendritic images were used for subsequent analysis only if the dendrites could be unambiguously traced to cells that excluded ethidium bromide and displayed no pathological changes (dendritic blebbing, swelling, etc.) throughout the duration of the experiment. Satisfactory dendrites were generally located at least 25 μm beneath the surface of the slice. Fluorescence of both DiI and ethidium bromide was excited by the 514 nm emission of a 25 mW argon ion laser. To minimize dye bleaching and phototoxicity, the laser intensity was reduced by 97% using a neutral density filter, and images were collected in photon-counting mode; 16 or 32 frames were averaged for each image to improve signal:noise. The confocal aperture was minimally opened, and serial optical sections were collected at 0.5 μm intervals through the region of interest (usually 20 serial sections). With 6× electronic zoom, the width of 1 pixel in the image corresponded to 0.08 μm in the object plane; images were 512 × 512 eight-bit pixels. In any one slice, serial optical sections were obtained from only one segment of secondary apical dendrite, 50–100 μm from its cell body.

Induction of long-term potentiation. Because electrical stimulation affects an indeterminate subset of synapses, we induced LTP by briefly exposing slices to a superfusate containing elevated Ca^{2+}, reduced Mg^{2+}, and tetraethylammonium (Turner et al., 1982; Bliss et al., 1984; Aniksztejn and Ben-Ari, 1991) in an effort to affect all potentiable synapses in the slice. Occlusion experiments and similarities of time course and pharmacological sensitivity indicate that such chemically induced LTP and electrically induced LTP share similar mechanisms (Bliss et al., 1986; Reymann et al., 1986; Cheng et al., 1994; Hanse and Gustafsson, 1994). After obtaining a first stack of serial optical sections through the selected dendritic segment, recording and stimulating electrodes were replaced on either side of the imaged area, and extracellular field potentials monitored. After 30 min of recording, long-term potentiation was induced in half of the slices by changing the superfusate from standard ACSF to a modified medium ("potentiation medium": 124 mM NaCl, 5 mM KCl, 1.25 mM KH_2PO_4, 24 mM $NaHCO_3$, 0.1 mM $MgCl_2$, 5 mM $CaCl_2$, 10 mM D-glucose and 25 mM tetraethylammonium chloride, pH 7.2) for 10 min, after which standard ACSF superfusion was continued for the remainder of the experiment. After 2.5 hr of electrical recording, and approximately 3.75 hr after obtaining the first images, a second stack of serial optical sections was obtained through the same dendritic segment, without changing the x-y position of the microscope stage. Slices exposed to potentiation medium were excluded from analysis if they did not sustain a stable increase in fEPSP slope that remained at least 20% above baseline at the end of the experiment.

Spine measurement and analysis. Pairs of image stacks were given coded labels to permit measurement by an observer without knowledge of whether a stack was from a first ("pre") or second ("post") imaging, or from a hippocampal slice exposed to potentiation medium ("potentiated") or only to standard ACSF ("control"). By moving up and down through the image stacks, dendritic spines could be unambiguously distinguished from dendritic branches, twists or kinks. Spine lengths were measured interactively on unprocessed confocal optical sections, using the Bio-Rad MRC-500 SOM program; three-dimensional reconstructions were not used for this purpose in order to avoid possible biases and nonlinear transformations implicit in the reconstruction procedure. For each spine, the optical section in each stack with the highest-contrast image of the extremity of that spine was identified; using that optical section, the cursor was then positioned alternately at the midpoint of the spine base and at the most distant margin of the spine. The distance between these points was taken as the "observed length" of the spine in that image stack. Thus, four groups of observed lengths (control "pre" and "post," and potentiated "pre" and "post") comprised a randomized blocks ANOVA design (Sokal and Rohlf, 1981).

"True," or three-dimensional, spine lengths were estimated by an unfolding analysis. The observed length of the spine represents a two-dimensional projection of the spine in the plane of section; the thickness of optical section, approximately 1.5 μm (full width at half-maximum) with the water-immersion objective used in these experiments, is sufficient to include the entire length of virtually all observed spines. (This section thickness is larger than the 0.5 μm interval between successive optical sections, so that all structures appeared in more than one section.) It is reasonable to assume that spines are randomly oriented with respect to the observer; it is then possible to estimate the distribution of true (3D) spine lengths, F, from the distribution of observed (2D projection) lengths, f, according to methods described previously (Rusakov, 1993; Rusakov and Stewart, 1995). Briefly, consider the distributions F and f as histograms having N length classes of width w, with true lengths denoted by $H(j) = jw$ ($j = 1,N$) and observed lengths denoted by $h(i) = iw$ ($i = 1,N$). For each individual spine, $h = H\sin\alpha$, where α is the angle between the spine axis and the line of sight. Then the chance of observing a given 2D projection length, iw, is the chance

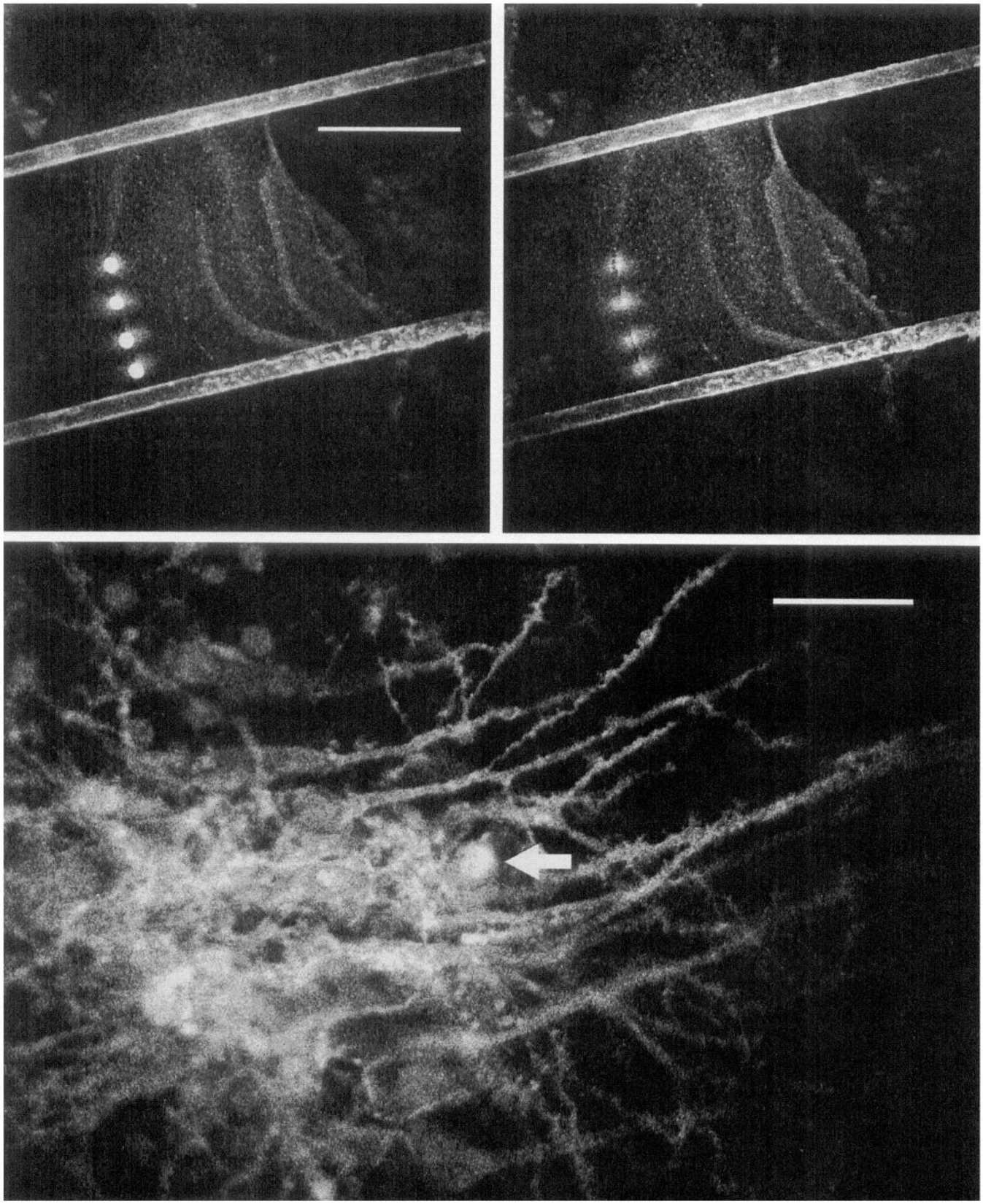

Figure 1. Focal application of DiI to a hippocampal brain slice via oil microdrops. *Top left*, Four microdrops have been placed along CA1 stratum pyramidale. *Top right*, The same slice, approximately 20 min later, after removal of dye microdrops from the brain slice. Remaining fluorescence at the prior locations of the microdrops is from small clusters of labeled cells. *Bottom*, Higher magnification confocal image a focally labeled CA1 site such as those in *Top right*. Numerous spine-laden dendrites emanate from the cluster of labeled cells. Ethidium bromide has entered a small

that some spine of true length jw is oriented at an angle of $\alpha = \arcsin(i/j)$. Because the chance of observing each 2D projection length is known from the experimental histogram f, and α is assumed to take values from 0 to π purely at random and independent of H, then estimating the frequency histogram F of 3D lengths represents a common inverse stereological problem (Coleman, 1989; Rusakov, 1993). The chance of observing each projection length is the sum of all possible 3D "events" that would give rise to it, that is, all possible true lengths and the corresponding values of $\sin\alpha = i/j$:

$$f(i) = A \sum_{j=1}^{N} F(j)\phi(i, j), \qquad i = 1, \ldots, N, \tag{1}$$

where A is a normalizer and $\phi(i, j)$ denotes the frequency distribution (i.e., the relative probabilities) of $\sin\alpha$. Because the frequency distribution of α is a constant (i.e., values of α are assumed to be uniformly distributed between 0 and π), the frequency distribution of $\sin\alpha$, that is $\phi(i, j)$, can be found numerically:

$$\phi(i, j) \cong jw^{-1} \{\arcsin(i/j) - \arcsin([i - 1]/j)\}$$

Then, given known experimental $f(i)$, and $\phi(i, j)$, Equation 1 can be solved for $F(i)$ using a "direct" recurrent formula as demonstrated previously (Rusakov, 1993):

$$F(i) = \left[f(i) - \sum_{j=i+1}^{J} F(j)\ \phi(i, j)\right] \phi(i, i)^{-1}, \quad i = J, J - 1, \ldots, 1. \tag{2}$$

Thus, the corresponding unknown distributions of 3D spine lengths, $F(i)$, were estimated from "pre" and "post" observations of control and potentiated groups. Further analysis was provided by Monte Carlo methods as described below.

Results

Analysis of observed spine lengths

Representative confocal optical sections through CA1 pyramidal cell dendritic segments from 15 potentiated and 11 control slices are shown in Figures 2 and 3, respectively, at the beginning and end of electrical recording sessions. Upon exposure to potentiation medium, fEPSP slope decreased slightly (79.8 ± 12.6% compared to baseline). When, after 10 min, slices were returned to standard ACSF, the fEPSP slope increased significantly beyond baseline levels (148.2 ± 0.6% compared to baseline, $P < 0.001$); this potentiation persisted in a stable manner throughout the remaining 2.5 hr of recording (Fig. 2). The slope of the fEPSP was unchanged in control slices maintained in standard ACSF throughout (Fig. 3).

Measurements were made before and after the induction of LTP ("pre" and "post" measurements, respectively) on 304 spines in the 15 slices that sustained LTP, and at corresponding intervals on 277 spines in the 11 control slices. The uncorrected mean spine density (visible spines per unit dendrite length, ±SEM) in the sample under study was 0.86 ± 0.07 spines/μm; there was no significant difference between potentiated and control slices. This value compares well with mean visible spine densities for CA1 apical dendrites measured by light microscopy in Golgi-impregnated material (Boublikova et al., 1991), indicating that our methods stain essentially all spines. The mean spine length in "pre" images did not significantly differ between potentiated (1.01 ± 0.25 μm variance) and control (1.06 ± 0.24 μm) groups. These values agree reasonably with previous measurements on fixed tissue (e.g., Horner and Arbuthnott, 1991), indicating that spines stained by our method are visible in their entirety.

New spines appeared infrequently along the dendritic segments over the 4 hr period of observation: we encountered only three instances of apparent spine formation among the 581 spines observed. These new spines appeared both in potentiated ($n = 1$) and control ($n = 2$) slices. No spines disappeared. The rarity of these events may be an artifact of our identification criteria: a spine that was small (and therefore difficult to discriminate) in one of the two image stacks and absent from the other would have been excluded from our counts. At the same time, it may be remarked that this rate, which corresponds to the emergence of approximately 0.03 new spines/μm/d, is compatible with observed increases in spine density during postnatal development (Juraska, 1982; Harris et al., 1992; Horner, 1993).

The results of Randomized Blocks ANOVA (paired comparison t test; Sokal and Rohlf, 1981) of observed spine lengths are summarized in Table 1. Small decreases in mean spine length from "pre" to "post" images were observed in the control group as well as in the potentiated group; these decreases were not statistically significant, nor was there a significant difference between the magnitude of these changes in the two groups. Equal means, however, do not imply the absence of significant differences between corresponding subpopulations of the two groups, since the component subpopulations of a group may display distinct behaviors. To examine this possibility, we performed more detailed statistical analyses.

Using the unfolding algorithm described in Materials and Methods, we estimated the "pre" and "post" distributions of true spine lengths, $F(i)$, for control (Fig. 4*C*) and potentiated (Fig. 4*D*) groups on the basis of the known distributions of observed spine lengths, $f(i)$ (Fig. 4*A,B*). Changes ("post" − "pre") in the relative frequencies of spines of each true length class could then be determined, and compared in potentiated versus control groups. The results of such a comparison (Fig. 5) suggest that potentiation is associated with a significant increase in the frequency of medium-length (1.0–1.4 μm) spines at the expense of smaller (0.6–0.8 μm) spines; such a shift can most easily be accounted for by growth of some of the smaller spines.

Changes in spine length versus initial spine length

Because in our experiments individual spines could be followed through time, change in spine length could be investigated directly. The plots in Figure 6 demonstrate explicitly the change in length of each spine versus its observed "pre" length. These plots reveal an unexpected phenomenon: the smallest spines apparently tend to grow, and large ones apparently tend to shrink, which is reflected in highly significant linear regressions (Fig. 6) that differ significantly between control and potentiated groups ($P < 0.04$, regression comparison according to Sokal and Rohlf, 1981).

These regression patterns might have reflected combinations of growth of smaller spines and a shrinkage of larger spines due to extensive deafferentation during slice preparation: reductions in overall spine density with increased numbers of short stubby spines, interpreted as evidence of spine shrinkage, have been seen by light microscopy of Golgi-impregnated material within 2 d of deafferenting lesions in hippocampus (Caceres and Stew-

←

number of cells, rendering their nuclei intensely fluorescent (*arrow*); most cells, including a majority of the DiI-labeled cells, are viable, showing only pale nuclear autofluorescence. This and all subsequent images were obtained with a 40× n.a. 0.75 water immersion objective. Scale bars: *Top left* and *Top right*, 1.0 mm; *Bottom*, 25 μm.

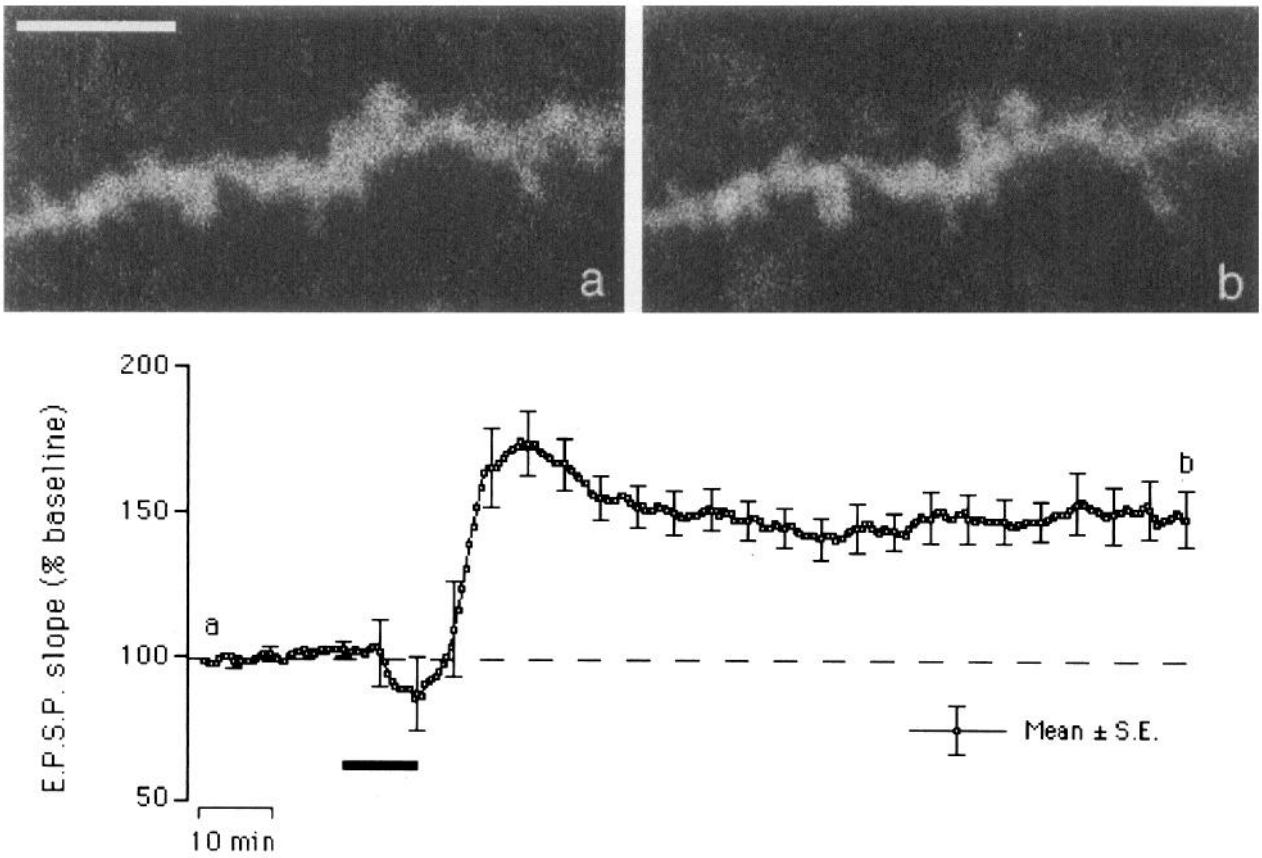

Figure 2. Evoked field excitatory postsynaptic potentials (fEPSPs) from slices undergoing potentiation, recorded in hippocampal CA1 stratum radiatum close to the imaging site. The graph at bottom shows the mean fEPSP slope for all potentiated preparations (n = 15), as a function of time; the stable increase in EPSP slope caused by 10 min exposure (*heavy bar*) to potentiation medium is apparent. Averaged, but otherwise unprocessed, confocal images of the same dendritic region, obtained at the beginning and end of a recording session, are shown above as *a* and *b*, respectively; scale bar is 5 μm. These images suffer from the unavoidable degradation associated with printed reproduction, but are otherwise typical of the resolution obtained in this study.

ard, 1983). However, the overall distributions of observed and 3D spine lengths (see above and Fig. 4) are not readily consistent with this hypothesis. Alternatively, the observed regression might result from small changes in spine orientation that could have occurred in the interval between obtaining the "pre" and "post" images. Because the observed length of a spine depends upon the angle between its axis and the observer's line of sight, changes in that angle would appear as changes in the spine's observed length, even if its true length remained constant (Fig. 7). To test whether such movement could account for the observed pattern of length changes, a Monte Carlo simulation was performed as follows.

Monte Carlo studies

Initially, 360 unitary segments (a number chosen to be compatible with the real experimental numbers) were oriented randomly with respect to an observer, and their observed (projection) lengths were determined. Then, the orientation of each segment was randomly deviated within a defined angular range ("rotation sector"), for example, ±5°, and the new projection length determined. Changes in projection length were plotted against initial projection length, as in Figure 6. The results of such simulations carried out for different rotation sectors (Fig. 8) clearly demonstrate that as permitted deviations increase, projection ("observed") length exhibits significant and increasingly steep linear regression with its own change. This regression resembles that of observed spine length in the experimental populations (Fig. 6), suggesting that random fluctuations in orientation of the spines are the main cause of the observed regression.

Since observed length data from control and potentiated groups yielded significantly different linear regression slopes (Fig. 6), we sought to determine whether this difference was due to differences in the range of angular deviations sustained by spines in control versus potentiated slices during the inter-imaging interval. To test this possibility, again Monte Carlo simulations were performed. Control and potentiated cases were modeled separately. In each case, initially 350 segments were generated, oriented randomly with respect to the viewer and with true lengths corresponding to the estimated distributions of true (three-dimensional) "pre" lengths for control or potentiated groups as in Figure 4, *C* and *D*. Observed lengths (i.e., projections) of the segments were calculated, yielding good fits, as expected, with the distributions of experimentally observed spine lengths. Then, in both groups, each segment underwent (1) a deviation in orientation, evenly randomly within a defined range, as described previously for the model in Figure 8; and (2) a change in length in order to fit the estimated distribution of true "post" length for that group as in Figure 4. Projections of the segments were then recalculated, and changes plotted as in Figure 6. For each group in each simulation experiment, the

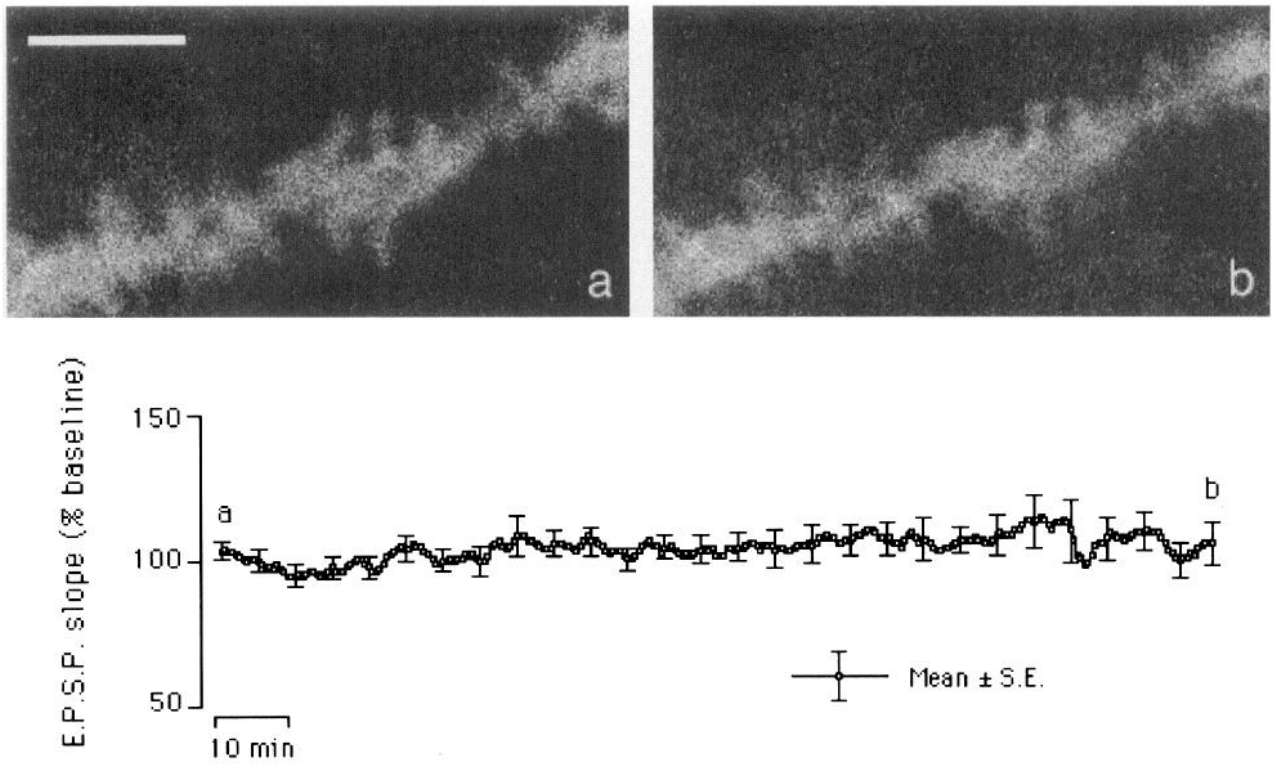

Figure 3. Confocal images and fEPSP analysis of control slices not exposed to potentiation medium. Representative "pre" and "post" confocal images and graph of fEPSP slope over time (mean of all control preparations, $n = 11$) are as in Figure 2.

rotation sector (i.e., the range of permitted deviation) was changed until the linear regression of modeled data and that of the experimental data (Fig. 6) achieved the best fit. The results of this simulation study are shown in Figure 9, and indicate that spines in potentiated slices undergo significantly greater angular deviations than control spines over similar periods.

Discussion

By use of confocal optics and oil microdrop application of DiI, fine details of neuronal structure can be imaged repeatedly in living brain slice preparations over periods of many hours without loss of cell viability. DiI and related carbocyanine dyes are well tolerated by cells, and fluorescent-labeled cells have normal physiological properties including synaptic transmission (Honig and Hume, 1986). These dyes have previously been microinjected in organic solvents to achieve discrete labeling of living nonmammalian neurons *in situ* (Liu and Westerfield, 1990; O'Rourke and Fraser, 1990; Danks et al., 1994), but such organic solvents, in our experience, cause unsatisfactory pathological changes in mammalian neurons. Using the present methods, we have previously established that individual dendritic spines persist and can be recognized over periods of hours (Hosokawa et al., 1992), a condition necessary if modulation of the strength of particular synapses serves as a basis for preservation of memories. The results reported here confirm those observations, and extend them by revealing changes in the length and motility of spines over such periods of time. Thus dendritic spines are *dynamic*, as well as persistent, structures. However, it is noteworthy that these morphological changes associated with LTP are small in magnitude. It should be borne in mind in this context that observing small dimensional changes of fluorescent structures presents a detection problem, and as such is information-limited rather than resolution-limited (Slayter and Slayter, 1992); with our system, changes as small as 0.1 μm can be detected, the significance of which must then be validated by statistical measures.

Our evidence that individual small dendritic spines increase in length in association with LTP (Fig. 5) is consistent with results of several electron microscopic analyses of fixed material. In their pioneering investigations of morphological correlates of LTP, Van Harreveld and Fifková (1975; Fifková and Van Harreveld, 1976) observed increases in the mean cross-sectional area of dentate granule cell dendritic spines in the distal molecular layer of potentiated rats; at poststimulation intervals equiv-

Table 1. ***ANOVA-Randomized-Blocks*** **(paired comparison) of the observed spine lengths**

Group of spines	Observed prelength (μm)	Observed postlength (μm)	Observed length change (μm)	*N*	*P*
Control	1.062 ± 0.236	1.056 ± 0.265	−0.006 ± 0.067	277	>0.39
Potentiated	1.013 ± 0.251	0.988 ± 0.223	−0.025 ± 0.074	304	

Means and variances are shown; *N*, total of spines in groups; *P*, significance level of the difference between spine length changes in control and potentiated groups (*F* test).

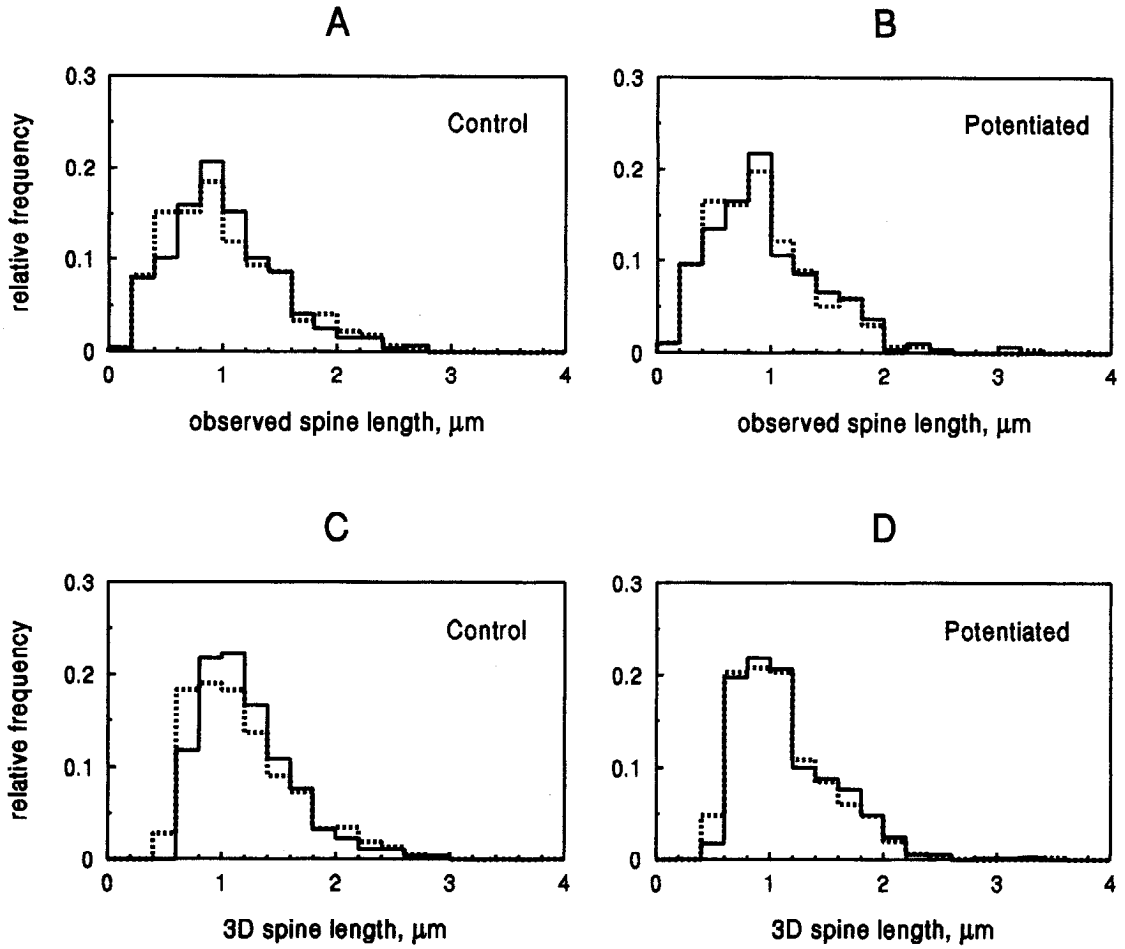

Figure 4. Frequency distribution histograms of observed spine lengths (*A, B*), and the estimated distributions of true (*3D*) spine lengths (*C, D*), for control (*A, C*) and potentiated (*B, D*) groups. *Solid lines* denote histograms of the initial ("pre") lengths, while *dotted line* denote histograms of spine lengths in "post" images.

alent to those in our experiments, spine area was increased by more than 35% compared to controls, and remained more than 20% above control values after 23 hr. Desmond and Levy (1983, 1986a) found a significant increase in the number of large spine profiles in the activated region of the rat dentate molecular layer in association with LTP. As in our study, the increase in number of large spine profiles was at the apparent expense of small spine profiles, leading Desmond and Levy to propose that potentiating stimulation causes growth ("interconversion") of existing, activated, spines. Desmond and Levy (1986b, 1988) also observed an increase in the apposed membrane surface area (including, but not limited to, an increase in the area of the postsynaptic

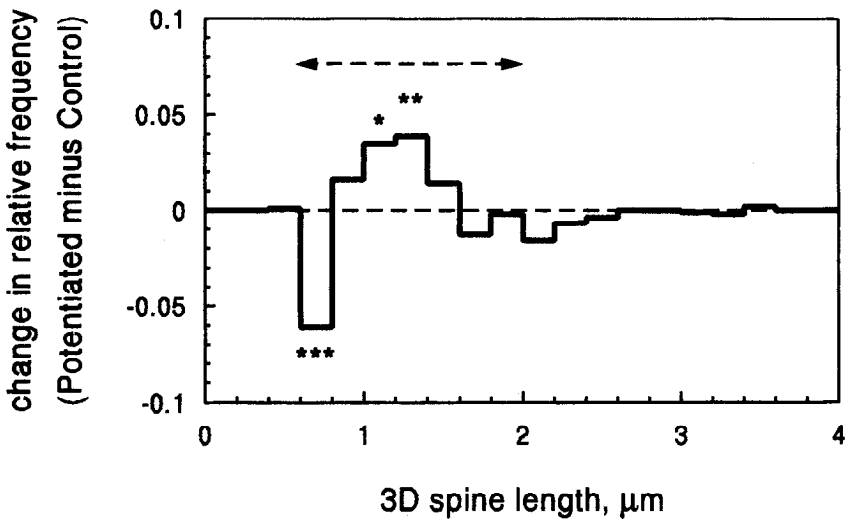

Figure 5. Histogram showing changes in relative frequency of spines of different initial 3D lengths, in potentiated versus control slices. The histogram was obtained by linear superposition of frequency histograms in Figure 4: ("post" potentiated − "pre" potentiated) − ("post" control − "pre" control). *Dashed line* marks the line representing the null hypothesis that there is no change, which is rejected for the histogram peaks labeled with asterisks (***, $P < 0.001$; **, $P < 0.007$; *, $P < 0.015$; determined by χ^2 analysis for the seven histogram bins that contained more than 10 spines in each of the four categories, as indicated by *dashed arrows*). Spines 1.0–1.4 μm in length become relatively more frequent after potentiation, mainly at the expense of smaller spines 0.6–0.8 μm in length, as compared to control slices.

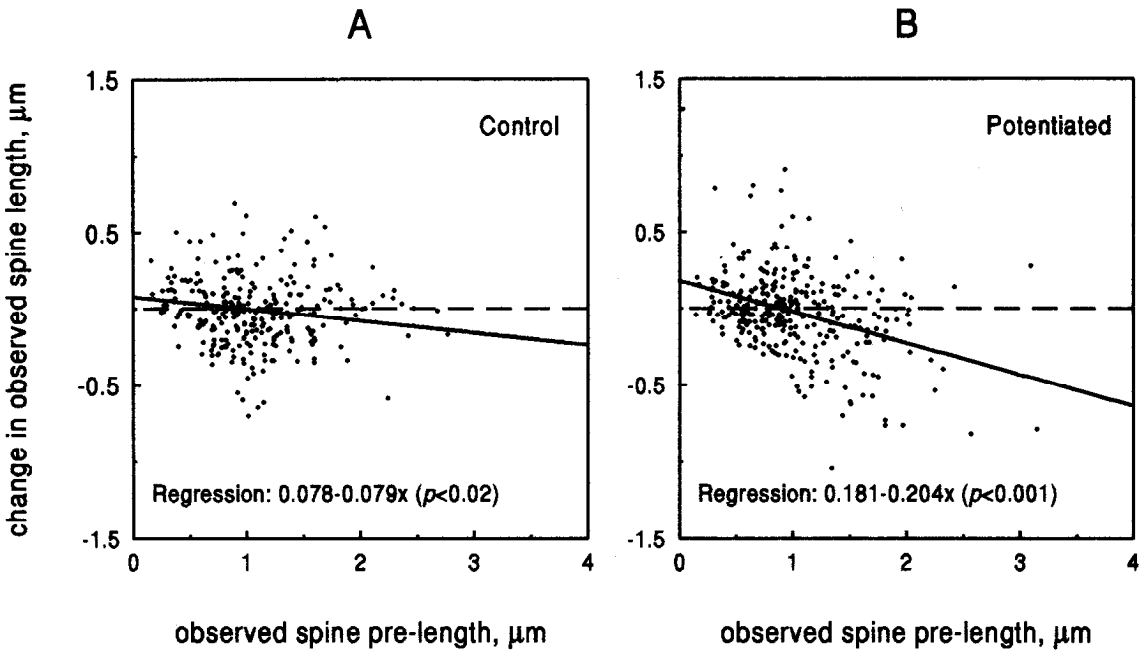

Figure 6. Change in observed length of individual CA1 pyramidal cell apical dendritic spines during the observation period, plotted against observed length of the spine measured at the beginning of experiments (*pre-length*). Control (*A*) and potentiated (*B*) hippocampal slices are plotted separately. Increases in observed length of smaller spines and decreases in observed length of larger spines are evident in both groups. *Dashes* mark zero-change lines; *solid lines* are linear regression fits of the data clouds. The regression equations and their significance levels are shown in the plots; the regression slopes in *A* and *B* differ significantly ($P < 0.04$).

density) in the subpopulation of spines whose frequency was increased by potentiating stimulation. All of these studies were based on individual thin sections, and therefore could not address spine length per se. However, Andersen et al. (1987a) and Trommald et al. (1990), on the basis of three-dimensional reconstructions from serial sections, found LTP in the dentate gyrus to be associated with elongation of spines, including both thickening and lengthening of the spine neck.

In contrast to these results in the dentate gyrus, Lee et al. (1979, 1980) and Chang and Greenough (1984) found no LTP-associated changes in spine area or postsynaptic density length in thin sections from rat CA1 stratum radiatum stimulated *in vitro* (although Chang and Greenough did observe significant rounding of spine heads at 10 min and 2 hr, but not 8 hr, after LTP, and not after nonpotentiating control stimulation). Rather, both groups reported a persistent increase in the number of synapses on dendritic shafts or small spines ["stubby" or "sessile" spines in the nomenclature of Jones and Powell (1969) and Harris et al. (1992)] per unit area of section. Chang et al. (1993) have, on this basis, inferred that "LTP in the hippocampus is related to synapse formation in CA1 and synapse shape change in the dentate gyrus."

In the present study, we found no association between potentiation and spine formation in CA1. Indeed, the formation of new spines appeared to be extremely rare events over our interval of observation. In addition, in contrast to previous suggestions (Nieto-Sampedro et al., 1982; Carlin and Siekevitz, 1983; Dyson and Jones, 1984; Trommald et al., 1990; Geinisman, 1991), we observed no splitting or bifurcation of preexisting spines with LTP. Nevertheless, our observations do not rule out

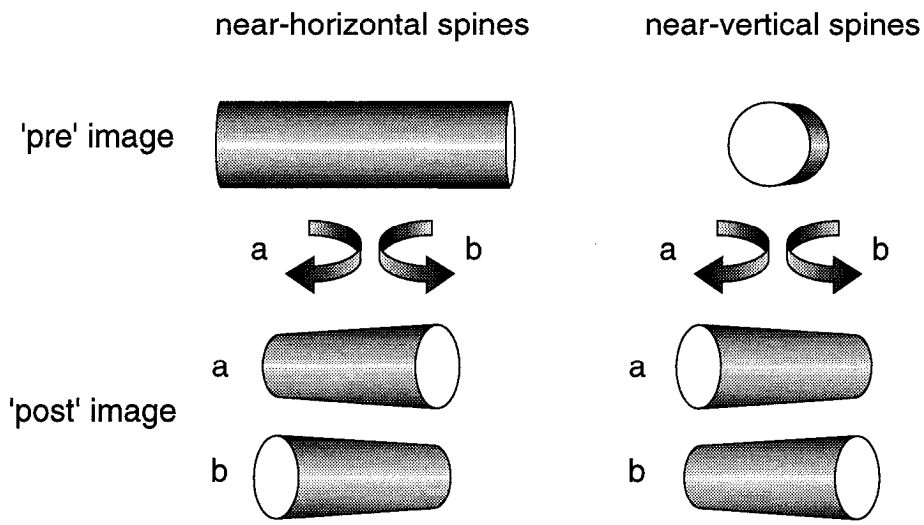

Figure 7. The observed length of spines will change between "pre" and "post" imaging sessions if the angle between the line of sight and the spine axis changes during that interval. Note that angular changes will generally cause those spines initially oriented perpendicular to the line of sight to appear to shrink (*left*) while causing spines initially oriented parallel to the line of sight to appear to grow (*right*).

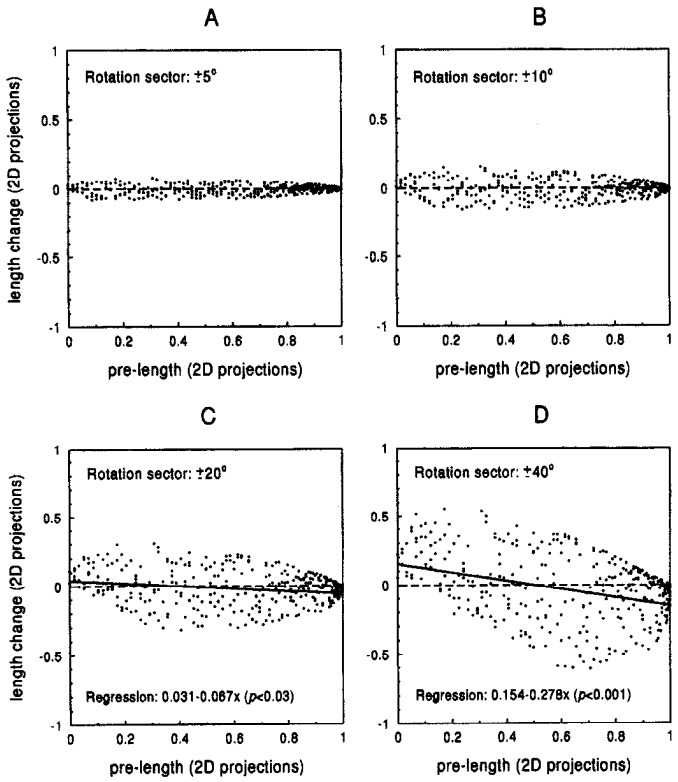

Figure 8. Results of Monte Carlo experiments in which a viewer measures the observed length (two-dimensional projections) of 360 segments of unit length having random initial orientations, and then measures the segments again after each has changed orientation randomly (with respect to the viewer) within a range ("rotation sector") of ±5° (*A*), ±10° (*B*), ±20° (*C*) or ±40° (*D*) of its initial orientation. Changes in observed length are plotted as in Figure 6. The data clouds in *C* and *D* exhibit significant linear regression (*straight lines*; equation shown in the plots), with *D* steeper than *C*.

the possibility of such potentiation-associated splitting or proliferation of spines or spine synapses. The spine size/transition frequency histogram (Fig. 5) that we observe implies that, under potentiating conditions, small spines are transformed into longer spines. However, our methods neglect shaft synapses and spines less than 0.2 μm long. Thus, potentiation-associated increases in numbers of shaft synapses such as reported by Lee et al. (1979, 1980) and by Chang and Greenough (1984) would be beyond our limit of detection. In addition, counts of spine synapses based on electron microscopic observations of single sections may increase if spines previously not in contact with presynaptic terminals (and thus not initially contributing to synapse counts) grow to contact nearby terminals (see below).

It has been suggested that similar growth of small spines may occur during development (Jones and Powell, 1969; Chang and Greenough, 1984; Steward et al., 1988; Harris et al., 1992). This raises the question of whether spine growth is an autonomous developmental process, or a consequence of learning during development. It may be relevant in this context that several reports based on Golgi staining suggest spine numbers are decreased by sensory deprivation, and are increased by exposure to enriched environments (reviewed by Horner, 1993); small spines may be undercounted in light microscopic studies of Golgi-impregnated material, so that shrinkage or growth of such spines may appear, respectively, as a decrease or increase in spine number. Our indications that LTP induction selectively lengthens small spines may also bear upon the observation that the extent of LTP obtainable in CA1 of rats peaks at 15 d of age (Teyler et al., 1989): at this age, a larger fraction of synapses are upon sessile (presumably small) spines than in adult animals (Harris et al., 1992); thus, if growth of this subset of spines contributes to expression of LTP, their greater relative abundance at 15 d could account for the developmental peak in LTP amplitude.

The growth of spines reported here appears to increase the proportion of large spines, but not to produce giant spines. Thus, whereas Andersen et al. (1987a), on the basis of three-dimensional reconstructions from serial electron microscopic sections, found that about 15% of dendritic spines of dentate granule cells in potentiated animals were longer than any in the control group, we observed no significant difference in the frequencies of the longest spines (>1.5 μm) between CA1 pyramidal neurons of potentiated versus control slices.

Our measurements, made before and 3.75 hr after induction of LTP, do not indicate how rapidly the observed changes in spine length occur; however, measurements on fixed material have suggested that activity-associated structural changes involving dendritic spines occur within the first 10 min—and possibly as early as the first 2 min—after stimulation (Van Harreveld and Fifková, 1975; Fifková and Van Harreveld, 1976; Lee et al., 1979; Chang and Greenough, 1984; Desmond and Levy, 1986a; Chang et al., 1993).

Problems of interpretation. Interpretation of our results depends upon the relationship between chemically induced LTP and more common forms of LTP such as that induced by tetanic electrical stimulation of the afferent pathway. In separate experiments using methods identical to those used here (Hosokawa et al., unpublished observations), we have determined that tetanic stimulation (three trains, 1 sec × 100 Hz, inter-train interval 5 sec) applied 60 min *after* inducing LTP by exposure to the chemical potentiation medium yielded no significant further potentiation at the CA3–CA1 synapse (EPSP slope 193.18 ± 16.44% of baseline after chemical potentiation, versus 233.22 ± 39.43% of baseline after further, tetanic, stimulation; $n = 4$, $P = 0.21$, paired t test); identical tetanic stimulation applied after similar delays to control slices not exposed to the chemical potentiation medium yielded significant LTP (EPSP slope 188.97 ± 21.45% of baseline; $n = 4$, $P < 0.01$). Such occlusion between chemically and electrically induced potentiation strongly suggests that both phenomena depend upon the same saturable mechanisms.

Our data suggest that in preparations undergoing potentiation, spine orientation changes to a significantly greater extent than in control preparations over similar intervals (see Fig. 9). The statistical analysis as well as the Monte Carlo simulations indicate that these changes and changes in spine length are not due to measurement errors but to real changes in the spines. The magnitude of the changes we report are likely to underestimate the actual changes at potentiated synapses, since even with chemical stimuli not all synapses in the slice are necessarily potentiated. Such changes could be artifacts of the experimental model (e.g., due to time-dependent changes in the mechanical properties of tissue slices, which may be enhanced by exposure to the potentiation medium independent of its effects on synaptic transmission). However, exposure to the potentiation medium in these experiments had no effect on somatic morphology, cell viability, or spontaneous activity; moreover, the significant difference in spine reorientation between control and potentiated preparations and the restriction of length changes to particular subsets of spines suggest that these spine changes reflect specific

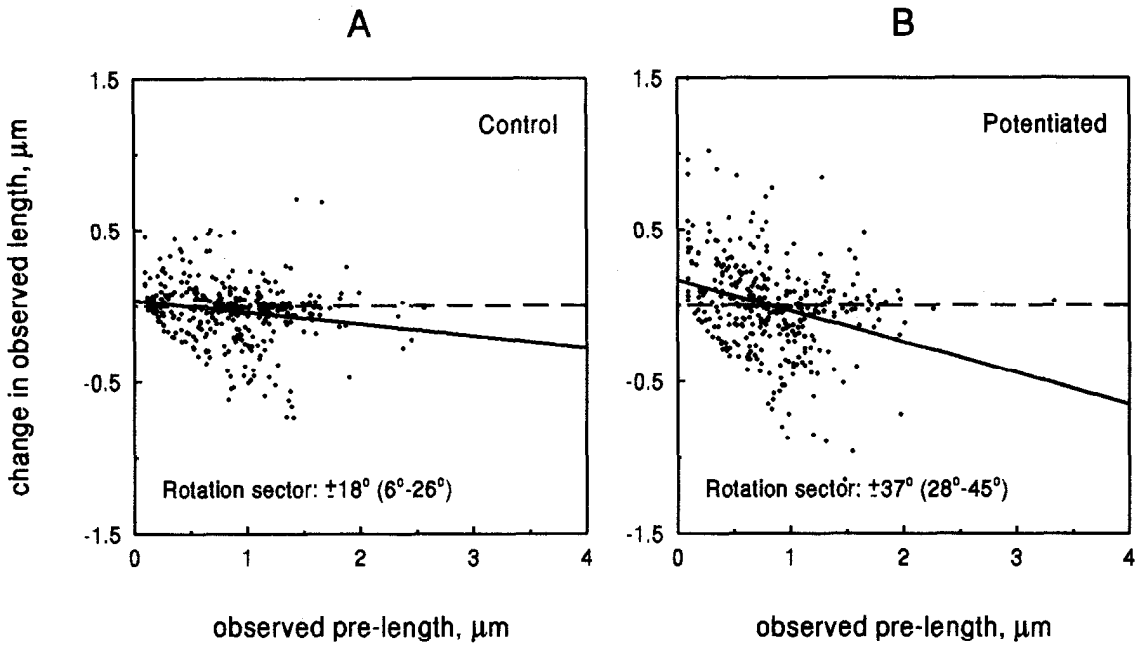

Figure 9. Monte Carlo simulation experiments in which the viewer measures the observed length (projection) of 350 different segments with uniformly random initial orientations, distributed in true length and rotated to fit the experimental data. In *A*, the segment lengths at the beginning of the experiment were distributed according to the estimated distribution of control-group three-dimensional spine "pre" lengths shown by the solid line histogram in Figure 4*C*; each segments then underwent a change in lengths to fit the distribution of control-group "post" lengths (dashed line histogram, Fig. 4*C*), and a random deviation in orientation within different ranges (rotation sectors) until the resulting regression fit the experimental regression of Figure 6*A*. The best-fit rotation sector is indicated in the plot, along with its 95% confidence interval in parentheses. In *B*, the same procedure has been carried out, using the potentiated-group data; the rotation sector best fitting the experimental regression of Figure 6*B* is shown. *Dashes* mark zero-change lines.

physiological effects of the potentiating stimulus. Biochemical mechanisms triggered by potentiating stimuli, such as protease activation (see below), would be expected to facilitate these changes. Furthermore, angular displacement may at least in part be a consequence of spine growth if such growth is constrained by adjacent structures.

We have interpreted our results as indicating that exposure to the potentiation medium causes changes both in spine length and orientation. We believe this to be the simplest and most plausible interpretation. However, it is in principle possible to explain our observations by orientation changes alone, if exposure to the potentiation medium induces orientational changes that are a particular function of spine length.

Mechanisms by which stimulation may induce postsynaptic morphological changes. Biochemical correlates of hippocampal LTP have been recently reviewed (Otani and Ben-Ari, 1993). Activity-dependent accumulation of calcium in dendritic spines has been observed in rapidly-frozen tissue by electron probe x-ray microanalysis (Andrews et al., 1988) and in living brain slice using fluorescent calcium indicators (Müller and Connor, 1991; Regehr and Tank, 1992). These intradendritic elevations in Ca^{2+} reflect calcium entry via synaptically activated NMDA-type glutamate receptors (Alford et al., 1993; Perkel et al., 1993), possibly amplified by influx through voltage-gated calcium channels and/or calcium-induced release of calcium from internal stores (Alford et al., 1993; Jaffe et al., 1994) such as the spine apparatus (Wilson et al., 1983). Siman et al. (1984) observed that brain spectrin (fodrin), a major component of the submembrane cytoskeleton and an actin- and calmodulin-binding protein, is degraded by the synaptosomal calcium-activated protease calpain I, and proposed that postsynaptic activity-induced calcium accumulation could, through this mechanism, alter the cytoskeleton leading to long-lasting changes in the shape of dendritic spines. By decreasing the rigidity of the spine, such cytoskeletal proteolysis could facilitate changes in spine orientation, such as those described here, that may be associated with modification of synaptic connections.

Spine reorientation and growth would also be facilitated by release or activation of extracellular proteases that could cleave the proteins stabilizing synaptic connections. Indeed, expression of one such protease, tissue plasminogen activator, has recently been found to increase early after LTP induction (Qian et al., 1993). Furthermore, levels of two membrane-spanning glycoproteins associated with maintenance of intercellular bonds, neural-cell adhesion molecule (NCAM) and amyloid precursor protein (APP), increase in push–pull superfusate of the dentate gyrus 90 min after induction of LTP (Fazeli et al., 1994).

Activity-dependent elevation of spine calcium levels would also be expected to activate two protein kinases that are components of the postsynaptic density, protein kinase C (PKC) and calcium/calmodulin dependent protein kinase II (CaMKII). Both kinases have been implicated in the induction of LTP (Lovinger et al., 1986, 1987; Silva et al., 1992). Among these enzymes' substrates are several cytoskeletal proteins found in dendritic spines, including the actin-binding proteins MAP-2 and myosin light chain. Changes in the spine actin network, resulting from phosphorylation of these proteins, have also been proposed as a basis for activity-dependent changes in spine morphology (Coss and Perkel, 1985; Fifkova, 1987; Fifkova and Morales, 1991). PKC appears to mediate the rapid and reversible growth of dendritic spinules associated with light adaptation in the mature retina (Weiler et al., 1991).

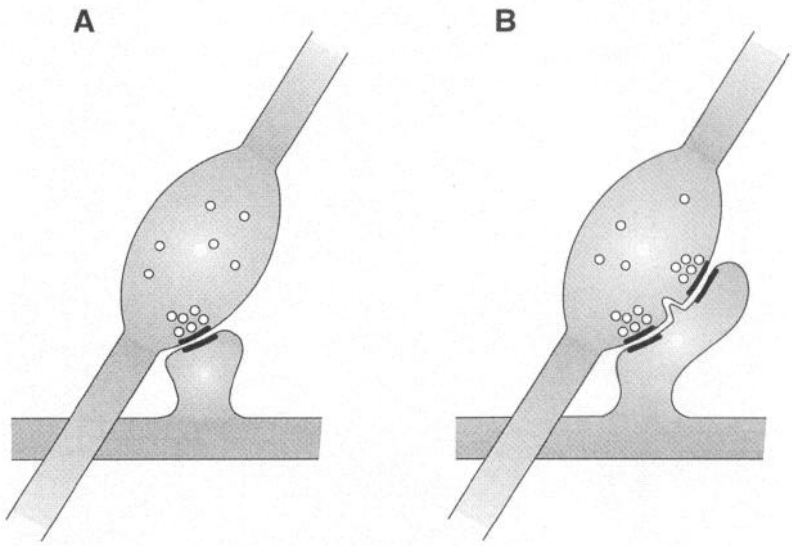

Figure 10. Spine growth from before (*A*) to after (*B*) induction of LTP may influence both "postsynaptic" and "presynaptic" quantal parameters. Such growth may be associated with insertion of additional postsynaptic receptors, and/or may be coupled to presynaptic changes such as addition of release sites and release apparatus. Alternatively, spine growth and/or displacement could permit receptor-bearing membrane to come into close contact with preexisting but ineffectual release sites, rendering them functional.

Several groups have obtained evidence for the selective accumulation of particular mRNAs in dendrites. Chicurel et al. (1993) found mRNA encoding GAP-43 and RC3 (both PKC substrates and calmodulin-binding proteins) to be selectively concentrated in a subcellular fraction enriched in dendritic spines (CA3 thorny excrescences). Kleiman et al. (1990), studying hippocampal cells in dissociated cell culture, found mRNA for the microtubule associated protein MAP-2, which is also an actin-binding protein, distributed throughout distal dendrites, although in these cultured cells GAP-43 mRNA appeared largely restricted to the soma and proximal dendrites. [Although GAP-43 protein is largely concentrated in axons, it has been detected immunohistochemically in the tips of dendritic spines (DiFiglia et al., 1990).] mRNA encoding the α-subunit of CaMKII has also been detected in distal dendrites (Burgin et al., 1990).

Synthesis of dendritic proteins, including components of the postsynaptic membrane, can be carried out locally in the dendrite (Rao and Steward, 1991; Torre and Steward, 1992) in a manner contributing to activity-dependent plasticity (Steward and Banker, 1992). Recently, it has been found that such dendritic protein synthesis may be activated by afferent stimulation: ^{3}H-leucine incorporation in CA1 dendrites is induced immediately after high frequency, but not low frequency, stimulation of Schaffer collaterals in the presence of carbachol (Feig and Lipton, 1993); label incorporation is blocked by D-aminophosphonovalerate and also by atropine.

Physiological consequences of spine plasticity. It has been suggested that dendritic spines serve to increase the available surface for synaptic contact, thereby permitting higher levels of neuronal connectivity (Ramon y Cajal, 1911; Swindale, 1981), or that they serve to restrict and amplify activity-induced calcium changes (Brown et al., 1988; Holmes, 1990). Although the dynamic LTP-associated changes in spine morphology described here are not incompatible with these proposed functions, they support the notion that structural plasticity of the dendritic spine serves as a basis for the maintained changes in synaptic strength necessary for lasting memories. Rall and Rinzel (1971) introduced the idea that changes in spine neck dimensions, leading to increased charge transfer from the synapse to the soma, could contribute to learning and memory; this possibility was considered in the original description of LTP (Bliss and Lømo, 1973). Computational studies suggest that such changes in spine neck dimensions, which are beyond the resolution of the present investigation, could indeed modulate quantal size if the spine membrane is excitable (Coss and Perkel, 1985; Perkel and Perkel, 1985; Shepherd et al., 1985; Brown et al., 1988; Koch et al., 1992); very recently, voltage-dependent calcium channels that could confer such excitability have been visualized on dendritic spines by confocal microscopy of fluorescent ligands (Mills et al., 1994). However, the equal sensitivity of potentiated and control synapses to experimental reduction in synaptic conductance has been taken as evidence against the hypothesis that changes in spine neck resistance are responsible for the expression of LTP (Jung et al., 1991).

Quantal analyses (Bekkers and Stevens, 1990; Malinow and Tsien, 1990; Larkman et al., 1992; Liao et al., 1992; Manabe et al., 1992; Voronin, 1993; Kullmann, 1994) have indicated that all of the statistical parameters of quantal transmission—quantal size, q; number of available release units, n; and probability of quantal release, P—may be altered in LTP. Morphological changes in dendritic spines could in principle affect any of these parameters (Carlin and Siekevitz, 1983; Harris and Stevens, 1989; Calverley and Jones, 1990; Edwards, 1991; Lisman and Harris, 1993; McNaughton, 1993; Bailey and Kandel, 1993). Thus, for example, if quantal release saturates available receptors at central synapses (Redman, 1990; Korn and Faber, 1991; Tong and Jahr, 1994), spine growth incorporating more postsynaptic receptors could yield increased q. Indeed, larger spines generally have larger postsynaptic densities and, presumably, more receptors and ion channels (Harris and Stevens, 1989; Lisman and Harris, 1993); increased size of the postsynaptic density has been reported by Desmond and Levy (1986b), as remarked earlier, in the subpopulation of large spines whose frequency is increased by LTP at the apparent expense of smaller spines. Alternatively, an increase in n or P—both widely considered presynaptic measures—might result from spine growth, if such growth lead to perforation of the postsynaptic density (Greenough et al., 1978) and/or coordinated changes in the presynaptic bouton (Desmond and Levy, 1986b; Schuster et al., 1990; Geinisman et al., 1992b; Lisman and Harris, 1993), or to receptor access to previously ineffectual transmitter release sites (Fig. 10). It has been suggested that the number and size of functional vesicular release sites increases in proportion with the size of the terminal bouton (Pierce and Lewin, 1994), and there is ev-

idence from fixed tissue of activity-dependent presynaptic structural changes in the hippocampus (Fifkova and Van Harreveld, 1977; Chang and Greenough, 1984; Applegate et al., 1987; Meshul and Hopkins, 1990; Represa and Ben-Ari, 1992). Note that physical coupling of pre- and postsynaptic membranes (postsynaptic densities are commonly observed bound to isolated synaptosomes) could obviate an obligatory role for diffusible retrograde messengers in triggering presynaptic expression of LTP (Lisman and Harris, 1993).

Implications for aging and dementia. The marked loss of dendritic spines in Alzheimer's disease and Down syndrome is well documented (Mehraein et al., 1975; Coleman and Flood, 1987; DeRuiter and Uylings, 1987; El Hachimi and Foncin, 1990; Ferrer and Gullotta, 1990; Baloyannis et al., 1992). Aging in rats, which is accompanied by impairments in learning, is also characterized by a substantial decrease in the frequency of axospinous synapses (Geinisman et al., 1992a). Some aspects of LTP-associated synaptic structural plasticity can still be observed in aged rats despite their reduced synaptic density (Geinisman et al., 1992b); in that study, however, no distinction was made regarding learning ability of the aged rats (Gage et al., 1984). It will be of interest to determine whether the ability to sustain activity-dependent spine growth is lost in aged, memory-impaired animals, thereby contributing to their functional impairment.

References

Alford S, Frenguelli BG, Schofield JG, Collingridge GL (1993) Characterization of Ca^{2+} signals induced in hippocampal CA1 neurons by the synaptic activation of NMDA receptors. J Physiol (Lond) 469: 693–716.

Andersen P, Blackstad T, Hullberg G, Trommald M, Vaaland JL (1987a) Dimensions of dendritic spines of rat dentate granule cells during long-term potentiation (LTP). J Physiol (Lond) 390:264.

Andersen P, Blackstad T, Hullberg G, Vaaland JL, Trommald M (1987b) Changes in spine morphology associated with LTP in rat dentate granule cells. Proc Physiol Soc PC50:288P.

Andrews SB, Leapman RD, Landis DMD, Reese TS (1988) Activity-dependent accumulation of calcium in Purkinje cell dendritic spines. Proc Natl Acad Sci USA 85:1682–1685.

Aniksztejn L, Ben-Ari Y (1991) Novel form of long-term potentiation produced by a K^+ channel blocker in the hippocampus. Nature 349: 67–69.

Applegate MD, Kerr DS, Landfield PW (1987) Redistribution of synaptic vesicles during long-term potentiation in the hippocampus. Brain Res 401:401–406.

Bailey CH, Kandel ER (1993) Structural changes accompanying memory storage. Annu Rev Physiol 55:397–426.

Baloyannis SJ, Manolidis SL, Manolidis LS (1992) The acoustic cortex in Alzheimer's disease. Acta Otolaryngol [Suppl] 494:1–13.

Bekkers JM, Stevens CF (1990) Presynaptic mechanisms for long-term potentiation in the hippocampus. Nature 346:724–729.

Bliss TVP, Collingridge GL (1993) A synaptic model of memory: long-term potentiation in the hippocampus. Nature 361:31–39.

Bliss TVP, Gardner-Medwin AR (1973) Long-lasting potentiation of synaptic transmission in the dentate area of the unanaesthetized rabbit following stimulation of the perforant path. J Physiol (Lond) 232: 357–374.

Bliss TVP, Lømo T (1973) Long-lasting potentiation of synaptic transmission in the dentate area of the anaesthetized rabbit following stimulation of the perforant path. J Physiol (Lond) 232:331–356.

Bliss TVP, Dolphin AC, Feasey KJ (1984) Elevated calcium induces a long-lasting potentiation of commissural responses in hippocampal CA3 cells of the rat *in vivo*. J Physiol (Lond) 350:65p.

Bliss TVP, Errington ML, Lynch MA (1986) Calcium-induced long-term potentiation in the dentate gyrus is accompanied by a sustained increase in transmitter release. In: Excitatory amino acid transmitters (Hicks TP, Lodge D, eds), pp 337–340. New York: Liss.

Boublikova L, Jiresova A, Pokorny J, Langmeier M, Trojan S (1991) Postnatal neuronal plasticity of the pyramidal cells of CA1 area of the hippocampus as a reaction to neurotoxic damage. Physiol Res 40: 585–593.

Brown TH, Chang VC, Ganong AH, Keenan CL, Kelso SR (1988) Biophysical properties of dendrites and spines that may control the induction and expression of long-term synaptic potentiation. In: Long-term potentiation: from biophysics to behavior (Landfield PW, Deadwyler SA, eds), pp 201–264. New York: Liss.

Burgin KE, Waxham MN, Rickling S, Westgate SA, Mobley WC, Kelly PT (1990) *In situ* hybridization histochemistry of Ca/calmodulin-dependent protein kinase in developing rat brain. J Neurosci 10: 1788–1798.

Caceres A, Steward O (1983) Dendritic reorganization in the denervated dentate gyrus of the rat following entorhinal cortical lesions: a Golgi and electron microscopic analysis. J Comp Neurol 214:387–403.

Calverley RKS, Jones DG (1990) Contributions of dendritic spines and perforated synapses to synaptic plasticity. Brain Res Rev 15:215–249.

Carlin RK, Siekevitz P (1983) Plasticity in the central nervous system: do synapses divide? Proc Natl Acad Sci USA 80:3517–3521.

Chang F-LF, Greenough WT (1984) Transient and enduring morphological correlates of synaptic activity and efficacy change in the rat hippocampal slice. Brain Res 309:35–46.

Chang F-LF, Hawrylak N, Greenough WT (1993) Astrocytic and synaptic response to kindling in hippocampal subfield CA1. I. Synaptogenesis in response to kindling *in vitro*. Brain Res 603:302–308.

Cheng G, Rong X-W, Feng T-P (1994) Block of induction and maintenance of calcium-induced LTP by inhibition of protein kinase C in postsynaptic neuron in hippocampal CA1 region. Brain Res 646:230–234.

Chicurel ME, Terrian DM, Potter H (1993) mRNA at the synapse: analysis of a synaptosomal preparation enriched in hippocampal dendritic spines. J Neurosci 13:4054–4063.

Coleman PD, Flood DG (1987) Neuron number and dendritic extent in normal aging and Alzheimer's disease. Neurobiol Aging 8:521–545.

Coleman R (1989) Inverse problems. J Microsc 153:233–248.

Colonnier M (1968) Synaptic patterns on different cell types in the different laminae of the cat visual cortex. An electron microscope study. Brain Res 9:268–287.

Coss RG, Perkel DH (1985) The function of dendritic spines—a review of theoretical issues. Behav Neurol Biol 44:151–185.

Danks AM, Kim P, Wang Z, Meyer RL (1994) Imaging of individual normal and regenerating optic fibers in the brain of living adult goldfish. J Comp Neurol 345:253–266.

DeRuiter JP, Uylings HBM (1987) Morphometric and dendritic analysis of fascia dentata granule cells in human aging and senile dementia. Brain Res 402:217–229.

Desmond NL, Levy WB (1983) Synaptic correlates of associative potentiation/depression: an ultrastructural study in the hippocampus. Brain Res 265:21–30.

Desmond NL, Levy WB (1986a) Changes in the numerical density of synaptic contacts with long-term potentiation in the hippocampal dentate gyrus. J Comp Neurol 253:466–475.

Desmond NL, Levy WB (1986b) Changes in the postsynaptic density with long-term potentiation in the dentate gyrus. J Comp Neurol 253: 476–482.

Desmond NL, Levy WB (1988) Synaptic interface surface area increases with long-term potentiation in the hippocampal dentate gyrus. Brain Res 453:308–314.

DiFiglia M, Roberts RC, Benowitz LI (1990) Immunoreactive GAP-43 in the neuropil of adult rat neostriatum: localization in unmyelinated fibers, axon terminals, and dendritic spines. J Comp Neurol 302: 992–1001.

Dyson SE, Jones DG (1984) Synaptic remodelling during development and maturation: junction differentiation and splitting as a mechanism of modifying connectivity. Dev Brain Res 13:125–137.

Eccles JC (1965) Possible ways in which synaptic mechanisms participate in learning, remembering and forgetting. In: The anatomy of memory (Kimble DP, ed), pp 97. Palo Alto: Science and Behaviour Books.

Edwards F (1991) LTP is a long term problem. Nature 350:271–272.

El Hachimi KH, Foncin J-F (1990) Perte des epines dendritiques dans la maladie d-Alzheimer. C R Acad Sci Paris 311[Serie III]:397–402.

Fazeli MS, Breen K, Errington ML, Bliss TVP (1994) Increase in

extracellular NCAM and amyloid precursor protein following induction of long-term potentiation in the dentate gyrus of anaesthetized rats. Neurosci Lett 169:77-80.
Feig S, Lipton P (1993) Pairing the cholinergic agonist carbachol with patterned Schaffer collateral stimulation initiates protein synthesis in hippocampal CA1 pyramidal cell dendrites via a muscarinic, NMDA-dependent mechanism. J Neurosci 13:1010–1021.
Ferrer I, Gullotta F (1990) Down's syndrome and Alzheimer's disease: dendritic spine counts in the hippocampus. Acta Neuropathol (Berl) 79:680–685.
Fifkova E (1987) Mechanisms of synaptic plasticity. In: Neuroplasticity, learning, and memory (Milgram NW, MacLeod CM, Petit TL, eds), pp 61–86. New York: Liss.
Fifkova E, Morales M (1991) The neuronal cytoskeleton and its possible role in synaptic plasticity. In: Development and plasticity of the visual system (Cronley-Dillon JR, ed), pp 133–147. London: Macmillan.
Fifkova E, Van Harreveld A (1977) Long-lasting morphological changes in dendritic spines of dentate granular cells following stimulation of the entorhinal area. J Neurocytol 6:211–230.
Fine A, Amos WB, Durbin RM, McNaughton PA (1988) Confocal microscopy: applications in neurobiology. Trends Neurosci 11:346–351.
Fine A, Hosokawa T, Bliss TVP (1991) Confocal imaging of changes in synaptic structure in living hippocampal slices. Soc Neurosci Abstr 17:1328.
Gage F, Kelly PAT, Bjorklund A (1984) Regional changes in brain glucose metabolism reflect cognitive impairments in aged rats. J Neurosci 4:2856–2865.
Geinisman Y, de Toledo-Morrell L, Morrell F (1991) Induction of long-term potentiation is associated with an increase in the number of axospinous synapses with segmented postsynaptic densities. Brain Res 566:77–88.
Geinisman Y, de Toledo-Morrell L, Morrell F, Persina IS, Rossi M (1992a) Age-related loss of axospinous synapses formed by two afferent systems in the rat dentate gyrus as revealed by the unbiased stereological dissector technique. Hippocampus 2:437–444.
Geinisman Y, de Toledo-Morrell L, Morrell F, Persina IS, Rossi M (1992b) Structural synaptic plasticity associated with the induction of long-term potentiation is preserved in the dentate gyrus of aged rats. Hippocampus 2:445–446.
Globus A (1975) Brain morphology as a function of presynaptic morphology and activity. In: The developmental neuropsychology of sensory deprivation (Riesen AH, ed), pp 9–91. New York: Academic.
Gould E, Woolley CS, Frankfurt M, McEwen BS (1990) Gonadal steroids regulate dendritic spine density in hippocampal pyramidal cells in adulthood. J Neurosci 10:1286–1291.
Greenough WT, Bailey CH (1988) The anatomy of a memory: convergence of results across a diversity of tests. Trends Neurosci 11: 142–147.
Greenough WT, West RW, DeVoogd TJ (1978) Subsynaptic plate perforations: changes with age and experience in the rat. Science 202: 1096–1098.
Hanse E, Gustafsson B (1994) TEA elicits two distinct potentiations of synaptic transmission in the CA1 region of the hippocampal slice. J Neurosci 14:5028–5034.
Harris KM, Kater SB (1994) Dendritic spines: cellular specializations imparting both stability and flexibility to synaptic function. Annu Rev Neurosci 17:341–371.
Harris KM, Stevens JK (1989) Dendritic spines of CA1 pyramidal cells in the rat hippocampus: serial electron microscopy with reference to their biophysical characteristics. J Neurosci 9:2982–2997.
Harris KM, Jensen FE, Tsao B (1992) Three-dimensional structure of dendritic spines and synapses in rat hippocampus (CA1) at postnatal day 15 and adult ages: implications for the maturation of synaptic physiology and long-term potentiation. J Neurosci 12:2685–2705.
Hebb DO (1949) The organisation of behaviour. New York: Wiley.
Holmes WR (1990) Is the function of dendritic spines to concentrate calcium? Brain Res 519:338–342.
Honig MG, Hume RI (1986) Fluorescent carbocyanine dyes allow living neurons of identified origin to be studied in long term cultures. J Cell Biol 103:171–187.
Horner CH (1993) Plasticity of the dendritic spine. Prog Neurobiol 41: 281–321.
Horner CH, Arbuthnott E (1991) Methods of estimation of spine density—are spines evenly distributed throughout the dendritic field? J Anat 177:179–184.
Hosokawa T, Bliss TVP, Fine A (1992) Persistence of individual dendritic spines in living brain slices. Neuroreport 3:477–480.
Hosokawa T, Bliss TVP, Fine A (1994) Quantitative three-dimensional confocal microscopy of synaptic structures in living brain tissue. Microsc Res Tech 29:290–296.
Ingham CA, Hood SH, Arbuthnott GW (1989) Spine density on neostriatal neurons changes with 6-hydroxydopamine lesions and with age. Brain Res 503:334–338.
Isokawa M, Levesque MF (1991) Increased NMDA responses and dendritic degeneration in human epileptic hippocampal neurons in slices. Neurosci Lett 132:212–216.
Jaffe DB, Fisher SA, Brown TH (1994) Confocal laser scanning microscopy reveals voltage-gated calcium signals within hippocampal dendritic spines. J Neurobiol 25:220–233.
Jones EG, Powell TPS (1969) Morphological variations in the dendritic spines of the neocortex. J Cell Sci 5:509–529.
Jung MW, Larson J, Lynch G (1991) Evidence that changes in spine neck resistance are not responsible for expression of LTP. Synapse 7:216–220.
Juraska JM (1982) The development of pyramidal neurons after eye opening in the visual cortex of hooded rats: a quantitative study. J Comp Neurol 212:208–213.
Kemp JM, Powell TPS (1971) The synaptic organization of the caudate nucleus. Philos Trans R Soc Lond [Biol] 262:403–412.
Kleiman R, Banker G, Steward O (1990) Differential subcellular localization of particular mRNA's in hippocampal neurons in culture. Neuron 5:821–830.
Koch C, Zador A, Brown TH (1992) Dendritic spines: convergence of theory and experiment. Science 256:973–974.
Korn H, Faber DS (1991) Quantal analysis and synaptic efficacy in the CNS. Trends Neurosci 14:439–445.
Kullmann DM (1994) Amplitude fluctuations of dual-component EPSCs in hippocampal pyramidal cells: implications for long-term potentiation. Neuron 12:1111–1120.
Larkman A, Hannay T, Stratford K, Jack J (1992) Presynaptic release probability influences the locus of long-term potentiation. Nature 360: 70–73.
Lee K, Oliver M, Schottler F, Creager R, Lynch G (1979) Ultrastructural effects of repetitive synaptic stimulation in the hippocampal slice preparation: a preliminary report. Exp Neurol 65:478–480.
Lee KS, Schottler F, Oliver M, Lynch G (1980) Brief bursts of high-frequency stimulation produce two types of structural change in rat hippocampus. J Neurophysiol 44:247–258.
Liao D, Jones A, Malinow R (1992) Direct measurement of quantal changes underlying long-term potentiation in CA1 hippocampus. Neuron 9:1089–1097.
Lisman JE, Harris KM (1993) Quantal analysis and synaptic anatomy—integrating two views of hippocampal plasticity. Trends Neurosci 16:141–147.
Liu DWC, Westerfield M (1990) The formation of terminal fields in the absence of competitive interactions among primary motoneurons in the zebrafish. J Neurosci 10:3947–3959.
Lovinger DM, Colley PA, Akers RF, Nelson RB, Routtenberg A (1986) Direct relation of long-duration synaptic potentiation to phosphorylation of membrane protein F1: a substrate for membrane protein kinase C. Brain Res 339:205–211.
Lovinger DM, Wong KL, Murakami K, Routtenberg A (1987) Protein kinase C inhibitors eliminate hippocampal long-term potentiation. Brain Res 436:177–183.
Malinow R, Tsien RW (1990) Presynaptic enhancement shown by whole-cell recordings of long-term potentiation in hippocampal slices. Nature 346:175–180.
Manabe T, Renner P, Nicoll RA (1992) Postsynaptic contribution to long-term potentiation revealed by the analysis of miniature synaptic currents. Nature 355:50–55.
Matthews DA, Cotman CW, Lynch G (1976) An electron microscopic study of lesion-induced synaptogenesis in the dentate gyrus. I. Magnitude and time course of degeneration. Brain Res 115:1–21.
McNaughton BL (1993) The mechanisms of expression of long-term enhancement of hippocampal synapses: current issues and theoretical implications. Annu Rev Physiol 55:375–396.
Mchracin P, Yamada M, Tarnowska-Dziduszko E (1975) Quantitative study of dendrites and dendritic spines in Alzheimer's disease and

senile dementia. In: Advances in neurology, Vol 12, Physiology and pathology of dendrites (Kreutzberg GW, ed), pp 453–458. New York: Raven.

Meshul CK, Hopkins WF (1990) Presynaptic ultrastructural correlates of long-term potentiation in the CA1 subfield of the hippocampus. Brain Res 514:310–319.

Mills LR, Niesen CE, So AP, Carlen PL, Spigelman I, Jones OT (1994) N-Type Ca^{2+} channels are located on somata, dendrites, and a subpopulation of dendritic spines on live hippocampal pyramidal neurons. J Neurosci 14:6815–6824.

Minsky M (1957) US Patent No. 3013467, granted 1961.

Müller M, Gähwiler BH, Rietschin L, Thompson SM (1993) Reversible loss of dendritic spines and altered excitability after chronic epilepsy in hippocampal cultures. Proc Natl Acad Sci USA 90:257–261.

Müller W, Connnor JA (1991) Dendritic spines as individual neuronal compartments for synaptic Ca^{2+} responses. Nature 354:73–76.

Nieto-Sampedro M, Hoff SW, Cotman CA (1982) Perforated postsynaptic densities: probable intermediates in synapse turnover. Proc Natl Acad Sci USA 79:5718–5722.

O'Rourke NA, Fraser SE (1990) Dynamic changes in optic fiber terminal arbors lead to retinotopic map formation: an *in vivo* confocal microscope study. Neuron 5:159–171.

Otani S, Ben-Ari Y (1993) Biochemical correlates of long-term potentiation in hippocampal synapses. Int Rev Neurobiol 35:1–41.

Parnavelas JG, Lynch G, Brecha N, Cotman CW, Globus A (1974) Spine loss and regrowth in hippocampus following deafferentation. Nature 248:71–73.

Perkel DH, Perkel DJ (1985) Dendritic spines: role of active membrane in modulating synaptic efficacy. Brain Res 325:331–335.

Perkel DJ, Petrozzino JJ, Nicoll RA, Connor JA (1993) The role of Ca^{2+} entry via synaptically activated NMDA receptors in the induction of long-term potentiation. Neuron 11:817–823.

Petukhov VV, Popov VI (1986) Quantitative analysis of ultrastructural changes in synapses of the rat hippocampal field CA3 *in vitro* in different functional states. Neuroscience 18:823–835.

Pierce JP, Lewin GR (1994) An ultrastructural size principle. Neuroscience 58:441–446.

Qian Z, Gilbert ME, Colicos MA, Kandel ER, Kuhl D (1993) Tissue-plasminogen activator is induced as an immediate-early gene during seizure, kindling and long-term potentiation. Nature 361:453–457.

Racine RJ, Milgram NW, Hafner S (1983) Long-term potentiation phenomena in the rat limbic forebrain. Brain Res 260:217–231.

Rall W, Rinzel J (1971) Dendritic spines and synaptic potency explored theoretically. Proc IUPS (XXV Intl Congr) IX:466.

Ramon y Cajal S (1891) Sur la structure de l'ecorce cerebrale de quelques mammiferes. Cellule 7:123–176.

Ramon y Cajal S (1911) Histologie du système nerveux de l'homme et des vertébrés, Vol II. Paris: Maloine.

Rao A, Steward O (1991) Evidence that protein constituents of postsynaptic membrane specializations are locally synthesized: analysis of proteins synthesized within synaptosomes. J Neurosci 11:2881–2895.

Redman S (1990) Quantal analysis of synaptic potentials in neurons of the central nervous system. Physiol Rev 70:165–198.

Regehr WG, Tank DW (1992) Calcium concentration dynamics produced by synaptic activation of CA1 hippocampal pyramidal cells. J Neurosci 12:4202–4223.

Represa A, Ben-Ari Y (1992) Kindling is associated with the formation of novel mossy fibre synapses in the CA3 region. Exp Brain Res 92: 69–78.

Reymann KG, Matthies HK, Frey U, Vorobyev VS, Matthies H (1986) Calcium-induced long-term potentiation in the hippocampal slice: characterization of the time course and conditions. Brain Res Bull 17:291–296.

Rusakov DA (1993) Estimation of the size distribution of closed cell elements from analysis of their random plane sections. Biometrics 49:141–149.

Rusakov DA, Stewart MG (1995) Quantification of dendritic spine populations using image analysis and a tilting dissector. J Neurosci Methods, in press.

Scheibel ME, Crandall PH, Scheibel AB (1974) The hippocampal-dentate complex in temporal lobe epilepsy. Epilepsia 15:55–80.

Schuster T, Krug M, Wenzel J (1990) Spinules in axospinous synapses of the rat dentate gyrus: changes in density following long-term potentiation. Brain Res 523:171–174.

Shepherd GM, Brayton RK, Miller JP, Segev I, Rinzel J, Rall W (1985) Signal enhancement in distal cortical dendrites by means of interactions between active dendritic spines. Proc Natl Acad Sci USA 82: 2192–2195.

Silva AJ, Stevens CF, Tonegawa S, Wang Y (1992) Deficient hippocampal long-term potentiation in α-calcium-calmodulin kinase II mutant mice. Science 257:201–206.

Siman R, Baudry M, Lynch G (1984) Brain fodrin: substrate for calpain I, an endogenous calcium-activated protease. Proc Natl Acad Sci USA 81:3572–3576.

Slayter EM, Slayter HS (1992) Light and electron microscopy. Cambridge: Cambridge UP.

Sokal RR, Rohlf FJ (1981) Biometry. San Francisco: Freeman.

Steward O, Banker GA (1992) Getting the message from the gene to the synapse: sorting and intracellular transport of RNA in neurons. Trends Neurosci 15:180–186.

Steward O, Davis L, Dotti C, Phillips L, Banker G (1988) Protein synthesis and processing in cytoplasmic microdomains beneath postsynaptic sites on CNS neurons: a mechanism for establishing and maintaining a mosaic postsynaptic receptive surface. Mol Neurobiol 2:227–261.

Swindale NV (1981) Dendritic spines only connect. Trends Neurosci 4:240–241.

Teyler TJ, Perkins AT, Harris KM (1989) The development of long-term potentiation in hippocampus and neocortex. Neuropsychologia 27:31–40.

Thanos S, Bonhoeffer F (1987) Axonal arborization in the developing chick retinotectal system. J Comp Neurol 261:155–164.

Tong G, Jahr CE (1994) Multivesicular release from excitatory synapses of cultured hippocampal neurons. Neuron 12:51–59.

Torre ER, Steward O (1992) Demonstration of local protein synthesis within dendrites using a new cell culture system that permits isolation of living axons and dendrites. J Neurosci 12:762–772.

Trommald M, Vaaland JL, Blackstad TW, Andersen P (1990) Dendritic spine changes in rat dentate granule cells associated with long-term potentiation. In: Neurotoxicity of excitatory amino acids (Guidotti AM, ed), pp 163–174. New York: Raven.

Turner RW, Baimbridge KG, Miller JJ (1982) Calcium-induced long-term potentiation in the hippocampus. Neuroscience 7:1497–1500.

Van Harreveld A, Fifková E (1975) Swelling of dendritic spines in the fascia dentata after stimulation of the perforant fibers as a mechanism of post-tetanic potentiation. Exp Neurol 49:736–749.

Voronin (1993) On the quantal analysis of hippocampal long-term potentiation and related phenomena of synaptic plasticity. Neuroscience 56:275–304.

Wallace CS, Hawrylak N, Greenough WT (1991) Studies of synaptic structural modifications after long-term potentiation and kindling: context for a molecular morphology. In: Long-term potentiation: a debate of current issues (Baudry M, Davis JL, eds), pp 189–232. Cambridge, MA: MIT Press.

Weiler R, Kohler K, Janssen U (1991) Protein kinase C mediates transient spinule-type neurite outgrowth in the retina during light adaptation. Proc Natl Acad Sci USA 88:3603–3607.

Wilson CJ, Groves PM, Kitai ST, Linder JC (1983) Three-dimensional structure of dendritic spines in the rat neostriatum. J Neurosci 3:383–398.

Wooley CS, Gould E, Frankfurt M, McEwen BS (1990) Naturally occurring fluctuation in dendritic spine density on adult hippocampal pyramidal neurons. J Neurosci 10:4035–4039.